The EMBO Journal (2005) 24, 4345–4355 | © 2005 European Molecular Biology Organization | All Rights Reserved 0261-4189/05
www.embojournal.org

THE EMBO JOURNAL

Distinct modes of ATR activation after replication stress and DNA double-strand breaks in *Caenorhabditis elegans*

Tatiana Garcia-Muse and Simon J Boulton*

DNA Damage Response Laboratory, Cancer Research UK, The London Research Institute, Clare Hall Laboratories, South Mimms, UK

ATM and ATR are key components of the DNA damage checkpoint. ATR primarily responds to UV damage and replication stress, yet may also function with ATM in the checkpoint response to DNA double-strand breaks (DSBs), although this is less clear. Here, we show that *atl-1* (*Caenorhabditis elegans* ATR) and *rad-5/clk-2* prevent mitotic catastrophe, function in the S-phase checkpoint and also cooperate with *atm-1* in the checkpoint response to DSBs after ionizing radiation (IR) to induce cell cycle arrest or apoptosis via the *cep-1*(p53)/*egl-1* pathway. ATL-1 is recruited to stalled replication forks by RPA-1 and functions upstream of *rad-5/clk-2* in the S-phase checkpoint. In contrast, *mre-11* and *atm-1* are dispensable for ATL-1 recruitment to stalled replication forks. However, *mre-11* is required for RPA-1 association and ATL-1 recruitment to DSBs. Thus, DNA processing controlled by *mre-11* is important for ATL-1 activation at DSBs but not following replication fork stalling. We propose that *atl-1* and *rad-5/clk-2* respond to single-stranded DNA generated by replication stress and function with *atm-1* following DSB resection.

The EMBO Journal (2005) **24,** 4345–4355. doi:10.1038/sj.emboj.7600896; Published online 1 December 2005
Subject Categories: genome stability & dynamics
Keywords: ATR; checkpoint; DSBs; replication stress

Introduction

In eukaryotic cells DNA-damage checkpoints sense the physical state of the genome and coordinate the orderly progression of the cell cycle with the completion of critical events such as DNA replication and repair (Shiloh, 2003; Kastan and Bartek, 2004). In response to DNA damage, checkpoint activation triggers a cascade of events that culminate in a transient cell cycle arrest, thus providing the necessary time for DNA repair to ensue. In metazoan organisms, checkpoint pathways can also induce apoptosis in the presence of irreparable or persistent DNA damage to eliminate compromised cells. The importance of DNA damage response (DDR) pathways in maintaining genomic integrity and preventing tumorigenesis is highlighted by the existence of inherited cancer predisposition syndromes, such as ataxia-telengiectasia (A–T) and Nijmegan breakage syndrome, which are caused by mutations in the checkpoint genes ATM and Nbs1, respectively (Carney *et al*, 1998; Shiloh, 2003).

ATM (ataxia-telangiectasia, mutated) and ATR (ATM and Rad3-related), members of the phosphatidylinositol 3-kinase related kinase (PIKK) family, are the primary sensors of DNA damage that are generally believed to function independently of each other in distinct DNA damage checkpoint signalling pathways (Abraham, 2001; Shiloh, 2003; Kastan and Bartek, 2004). Indeed, ATM and ATR primarily respond to different types of DNA damage and exhibit distinct differences in how they are recruited and activated by DNA lesions (Falck *et al*, 2005). ATM responds to the presence of DNA double-strand breaks (DSBs) generated following ionizing radiation (IR)-treatment and is activated by autophosphorylation on Ser-1981 (Bakkenist and Kastan, 2003) prior to its recruitment to DSBs through an interaction with the Mre11–Rad50–Nbs1 (MRN) complex (Costanzo *et al*, 2004; Falck *et al*, 2005; Lee and Paull, 2005). ATR on the other hand primarily responds to DNA lesions generated following replication fork stalling in S-phase or following UV damage (Kastan and Bartek, 2004). Accumulation of RPA bound to single-stranded DNA (ssDNA) generated during DNA lesion processing or following replication stress are believed to recruit and activate ATR via its interacting partner, ATRIP (Zou and Elledge, 2003).

Once activated ATM and ATR trigger checkpoint responses by phosphorylating distinct as well as overlapping downstream target proteins, such as Chk1, Chk2 and p53 to bring about cell cycle arrest, DNA repair or apoptosis (Durocher and Jackson, 2001; Kastan and Bartek, 2004). Although ATM and ATR are primarily activated by different DNA lesions, placing them into separate checkpoint pathways maybe an oversimplification as ATR can compensate for loss of ATM under certain conditions. For example, overexpression of ATR can partially restore radio-resistance to A–T cells, phosphorylation of p53 and Chk1 after IR-treatment is delayed rather than abolished in A–T cells, and overexpression of a dominant-negative kinase dead mutant of ATR confers defects in cell cycle checkpoint activation in response to DSBs generated following IR (Cliby *et al*, 1998; Wright *et al*, 1998; Kastan and Bartek, 2004). Collectively, these observations suggest that ATR may participate with ATM in the checkpoint response to DSBs. In the absence of ATR-deficient cells that survive in culture (Brown and Baltimore, 2000), it has been difficult to determine the importance of ATR in the checkpoint response to DSBs. However, it may be possible to analyze the role of ATR in the DSB response in cell lines carrying hypomorphic mutations in ATR that were derived from two related Seckel syndrome patients (O'Driscoll *et al*, 2003).

*Corresponding author. DNA Damage Response Laboratory, Cancer Research UK, The London Research Institute, Clare Hall Laboratories, Blanche Lane, South Mimms, Herts EN6 3LD, UK.
Tel.: +44 1707 625774; Fax: +44 2072 693801;
E-mail: simon.boulton@cancer.org.uk

Received: 30 August 2005; accepted: 10 November 2005; published online: 1 December 2005

Several features of the *Caenorhabditis elegans* adult hermaphrodite germline, required for generating haploid gametes, make it a powerful model for dissecting the underlying mechanisms required for the DDR. Each germline is spatially polarized in a distal-to-proximal manner with respect to mitotic proliferation and progression through meiotic prophase I. Following the detection of DNA damage, conserved DNA damage checkpoint pathways transduce signals to the cell cycle machinery to induce arrest of mitotically dividing cells, or to the apoptosome to induce death of pachytene cells (Gartner *et al*, 2000; Boulton *et al*, 2002). Currently, *rad-5/clk-2* is the only *C. elegans* gene shown to be essential for the S-phase checkpoint, but how *rad-5/clk-2* performs its functions is not known (Ahmed *et al*, 2001). The *C. elegans* 9-1-1 complex components, *mrt-2* (ScRad17/SpRad1) and *hus-1,* together with *rad-5/clk-2*, are required for IR-induced cell cycle arrest and germ cell death, yet are surprisingly dispensable for the S-phase checkpoint (Ahmed and Hodgkin, 2000; Ahmed *et al*, 2001; Boulton *et al*, 2002; Hofmann *et al*, 2002). It is currently unclear how checkpoint activation brings about cell cycle arrest in the mitotic compartment of the germline. However, like in mammals, checkpoint activation in response to IR triggers germ cell death by activating the *C. elegans* p53 homolog (CEP-1) that induces expression of the BH3 domain containing protein, EGL-1, that in turn regulates the general cell death regulators, CED-3 and CED-4 (Conradt and Horvitz, 1998; Derry *et al*, 2001; Hengartner, 2001; Schumacher *et al*, 2001, 2005).

Here we report the characterization of a mutant in the *C. elegans* homolog of ATR (*atl-1*). Although *atl-1* is essential, maternal rescue permits analysis of *atl-1* loss-of-function in adult tissues. Both *atl-1* and *rad-5/clk-2* mutants exhibit mitotic catastrophe and defects in the S-phase checkpoint. ATL-1 is recruited to stalled replication forks by RPA-1 bound to ssDNA and functions upstream of RAD-5/CLK-2 in the checkpoint pathway. Surprisingly, we find that *atl-1*, as well as *atm-1* and *rad-5/clk-2,* are required for checkpoint dependent cell cycle arrest and apoptosis via the *cep-1/egl-1* pathway in response to DSBs generated by IR. ATL-1 recruitment to DSBs also requires *rpa-1*, but unlike its recruitment to stalled replication forks, there is an additional requirement for *mre-11*. The failure to recruit ATL-1 to DSBs in the absence of *mre-11* is due to a defect in processing DBSs to generate resected ssDNA ends bound by RPA-1. Thus, ATL-1 and RAD-5/CLK-2 function in S-phase checkpoint and ensure replication fork stability, and also cooperate with ATM-1 in the checkpoint response to DSBs.

Results

C. elegans ATR is essential for viability

The lack of ATR-deficient animals or cells has been an obstacle to functional studies of this gene as knockout mice are embryonic lethal (Brown and Baltimore, 2000; de Klein *et al*, 2000), cells generated from these mice fail to survive in culture and analysis of ATR-deficient cells generated by siRNA or cre-lox excision of ATR is restricted to one cell division (Cortez *et al*, 2001). We reasoned that analysis of ATR loss-of-function might be possible in *C. elegans* as many lethal mutations can be studied in homozygous progeny, if rescued into adulthood by maternal mRNA contribution.

atl-1, the *C. elegans* homolog of ATR, is located at the T06E4.3 locus on chromosome V. The *atl-1* gene spans 10.47 kb, including 18 exons, and is predicted to encode two splice variants, T06E4.3a and T06E4.3b, that produce 2531 and 2514 amino-acid proteins, respectively (Figure 1A and B). The function of the two predicted isoform's is currently unknown but both possess extensive sequence conservation throughout all known functional domains in human ATR, displaying 20% identity and 36% similarity in the FAT domain, 39% identity and 57% similarity in the phosphatidylinositol 3- and 4-kinase catalytic motif (PI3Kc) and 36% identity and 50% similarity in the FATC domain compared with the corresponding regions of human ATR (Figure 1A). In *C. elegans* there is another member of the PI3Kase family called *atm-1*, with high homology to HsATM (Supplementary Figure S1A).

We have characterized an *atl-1* deletion mutant allele, *atl-1(tm853)*, that was isolated by PCR using *atl-1* specific primers from a UV-trimethylpsoralen mutagenized library. A 720 bp region within exon 7 of the T06E4.3 locus is deleted in *atl-1(tm853)* creating a frameshift in the *atl-1* gene that results in a premature stop codon, which prevents expression of the last 12 exons, including the FAT, PI3Kc kinase and FATC domains (Figure 1B and C). The *atl-1(tm853)* allele is predicted to encode a 479 amino-acid truncated product. This product is undetectable by Western blotting and is unlikely to function as a dominant negative as *atl-1(tm853)/+* heterozygotes are viable and exhibit wild-type responses to DNA damage (Supplementary Figure S2). The major phenotype associated with depletion of *atl-1* using RNA-mediated interference (RNAi) is a Him (high incidence of males) phenotype, reflecting chromosome segregation defects, and partial lethality during early embryogenesis, explained in part, by a cell-cycle timing defect during early development (Aoki *et al*, 2000; Brauchle *et al*, 2003). In contrast, *atl-1(tm853)* confers complete embryonic lethality (Emb phenotype), suggesting that RNAi depletion of *atl-1* does not necessarily reflect complete loss-of-function for this gene. Although the brood size produced by *atl-1(tm853)* mutant animals is similar to wild-type of 817 embryos analyzed from *atl-1(tm853)* animals none survived, whereas 852 embryos analyzed from wild-type (N2) worms all survive to adulthood (Figure 1D). These findings suggest that as in mice (Brown and Baltimore, 2000; de Klein *et al*, 2000), *atl-1* is an essential gene in *C. elegans* and is required for completion of embryogenesis.

atl-1 and rad-5/clk-2 prevent mitotic catastrophe

Although *atl-1* is an essential gene, *atl-1(tm853)/+* heterozygous hermaphrodite parents produce *atl-1(tm853)* homozygous progeny by self-fertilization. These progeny are rescued through to adulthood by maternal mRNA contribution, thus permitting analysis of *atl-1* loss-of-function within adult tissues. *atl-1(tm853)* adult hermaphrodites display normal locomotion, touch responses, pharyngeal pumping, egg laying and overall morphology, suggesting that *atl-1* is dispensable for generating functional somatic tissues during development (data not shown). The *C. elegans* hermaphrodite germline is responsible for generating germ cells and is spatially polarized in a distal-to-proximal manner with respect to mitotic proliferation and progression through meiotic prophase (Figure 2A). The distal end of the germline comprises a stem cell compartment of mitotically proliferating nuclei that are followed, more proximally, by cells in pro-

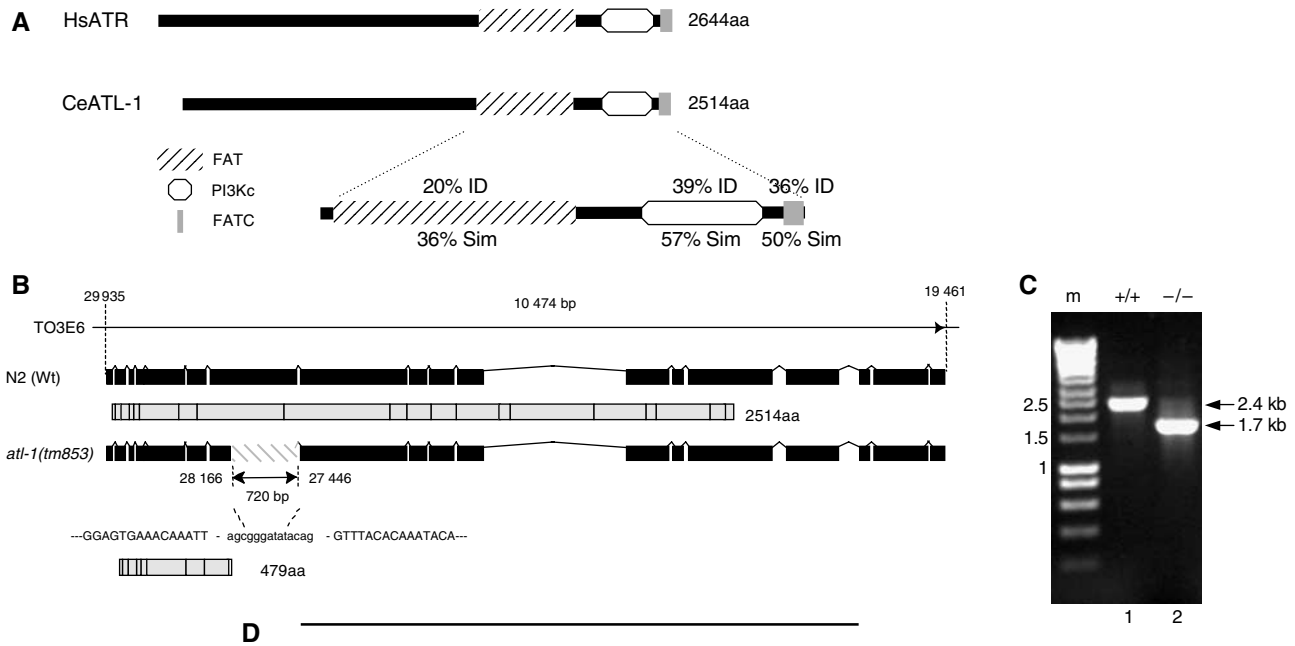

D

atl-1 mutants exhibit embryonic lethality

Genotype	Total eggs	Viable progeny	Percent lethality
N2	852	852	0
atl-1(tm853)[a]	817	0	100

Figure 1 Mutation in *atl-1*, the *C. elegans* homolog of ATR, results in embryonic lethality. (**A**) Schematic representation of *C. elegans atl-1* compared with *H. sapiens* ATR. The various conserved domains positions, including the FAT domain (diagonal stripes box), the PI3K domain (white box) and the FATC domain (gray box), and their respective identity (ID) and similarity (Sim) compared to HsATR are indicated. (**B**) Schematic of *atl-1* gene structure and the predicted protein product for wild-type (Wt) N2 (2514aa protein) and the *atl-1(tm853)* deletion mutant (479aa predicted). *atl-1(tm853)* carries a 720 bp deletion in the 7th exon that generates a premature stop codon. The numbers indicates the nucleotide positions in the cosmid T03E6. (**C**) Nested PCR with *atl-1* specific primers from a single wild-type N2 worm (lane1) and a single *atl-1 (tm853)* mutant worm (lane 2) showing the 720-bp deletion. (**D**) Embryonic lethality was scored by counting the number of eggs laid (Total Eggs), which was compared to the number of eggs that hatch to produce viable progeny. [a]The hermphrodites whose progeny were scored in these experiments were homozygous *atl-1* mutants derived from *atl-1* $-/+$ parents.

gressive stages of meiosis I. It is possible to distinguish nuclei in the mitotic zone from those in the early stages of meiosis I by the characteristic transition to 'crescent-shaped' nuclei that define the initial stages of homolog alignment and pairing in early meiosis.

Cytological analysis of fixed germlines isolated from *atl-1(tm853)* mutants reveals a highly disorganized mitotic zone with aberrant nuclei and evidence of chromosomal aberrations resembling the mitotic catastrophe and nuclear fragmentation phenotype described for $ATR^{-/-}$ cells (Brown and Baltimore, 2000; Alderton *et al*, 2004) (Supplementary Figure S1B). Unlike wild-type (N2) worms, *atl-1* mutants exhibit regions of ssDNA and multiple DSBs in mitotic germline nuclei, as indicated by the presence of multiple replication protein A (RPA-1) and RAD-51 nuclear foci, respectively (Figure 2B) (Martin *et al*, 2005). Early meiotic nuclei, distinguished from mitotic nuclei by their 'crescent-shaped' appearance, are devoid of detectable RPA-1 and RAD-51 staining in *atl-1* mutants, indicating that the genome instability resulting from the loss of ATL-1 arises in mitotic nuclei.

The *mn159* mis-sense allele in the *rad-5/clk-2* checkpoint gene is viable at 15°C but confers a temperature-sensitive embryonic lethal phenotype when grown at the restrictive temperature of 25°C (Ahmed *et al*, 2001). Although no obvious defects were observed in the first two embryonic cell division in *rad-5(mn159)* mutants following a shift to the nonpermissive temperature, it is possible that the lethality observed at 25°C could be caused by a defect during S-phase (Ahmed *et al*, 2001). Indeed, L4 stage *rad-5(mn159)* mutants shifted to the nonpermissive temperature of 25°C for 12 h exhibit a dramatic accumulation of single stranded DNA and DSBs that are restricted to cells undergoing S-phase in the mitotic compartment of the germline (Figure 2B). This phenotype is very similar to that observed in *atl-1* mutants, implying that *atl-1* and *rad-5/clk-2* may function in a common pathway to prevent mitotic catastrophe and genome instability in S-phase cells. These observations are consistent with the proposed role for ATR in stabilizing stalled replication forks and also implicate RAD-5/CLK-2 in promoting fork stability (Lopes *et al*, 2001; Tercero and Diffley, 2001; Shechter *et al*, 2004).

atl-1 is dispensable for SC assembly and crossover recombination during meiotic prophase

Following exit from the mitotic cell cycle and completion of premeiotic S-phase, homologs align, 'zip' together (synapsis)

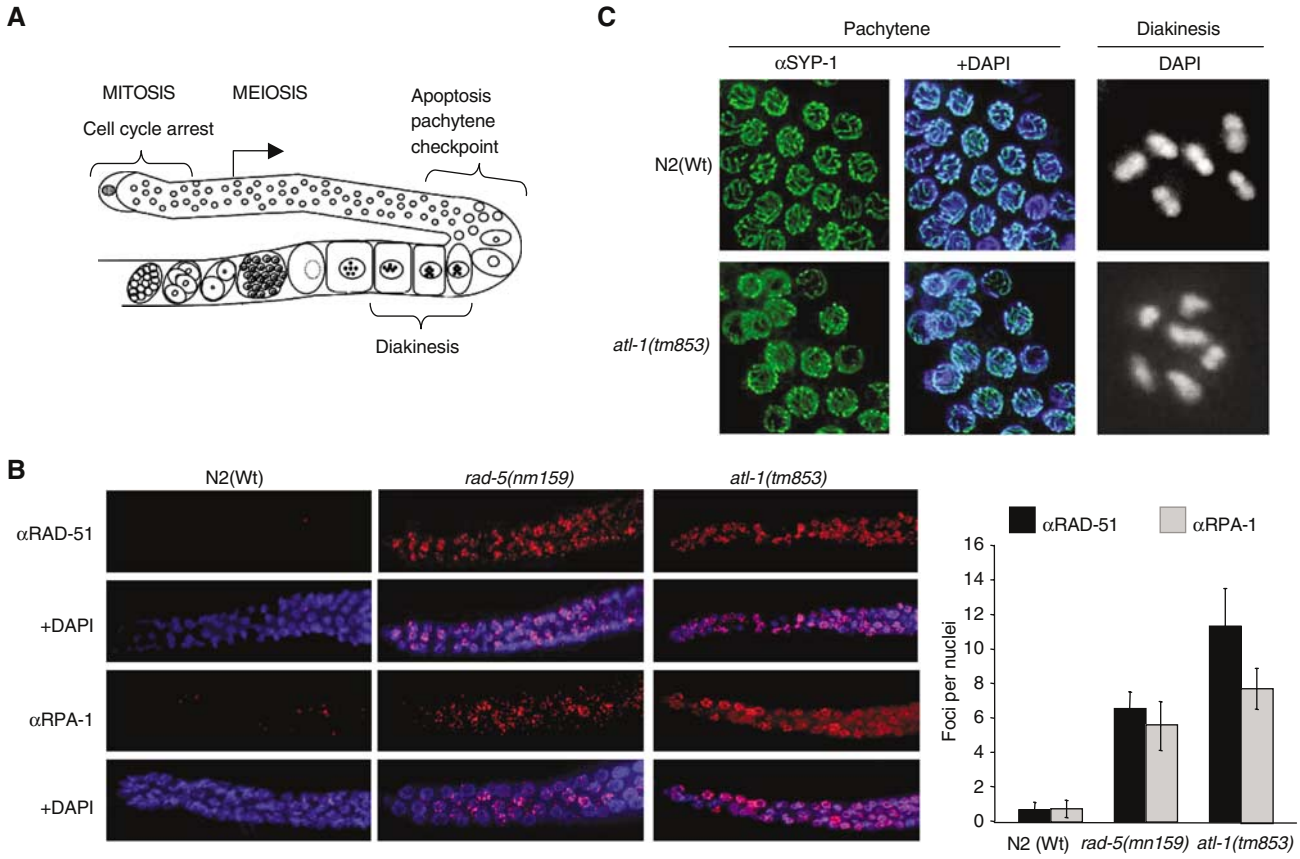

Figure 2 *atl-1* inactivation leads to mitotic catastrophe but is dispensable for meiotic prophase I. (**A**) Diagram of the adult *C. elegans* hermaphrodite gonad. In wild-type animals, genotoxic stress leads to checkpoint-dependent cell cycle arrest of nuclei in the mitotic compartment and apoptosis of meiotic germ cells via the pachytene checkpoint (Gartner *et al*, 2000). (**B**) Representative images of fixed germlines of the indicated genotype immunostained with RPA-1 and RAD-51 antibodies and counterstained with DAPI. Wild type (N2) and *atl-1* mutant worms were analyzed under normal growth at 20°C, *rad-5(mn159)* was analyzed after growth at the nonpermissive temperature of 25°C. Quantification of the number of RPA-1 and RAD-51 foci per nucleus for the indicated genotypes is shown in the graph on the right. Error bars indicate standard error of mean from at least 20 nuclei from 10 to 15 worms of each genotype. (**C**) Representative images of fixed pachytene nuclei from N2(Wt) and *atl-1(tm853)* mutants immunostained with the core SC component, SYP-1 (MacQueen *et al*, 2002). Representative images of a single oocyte nucleus arrested at diakinesis counterstained with DAPI from N2(Wt) and *atl-1(tm853)* mutants.

and are held in place along their entire length by a protein/DNA structure called the synaptonemal complex (SC). Although the mitotic zone is severely compromised in *atl-1* mutants, meiotic prophase nuclei are cytologically normal and correctly assemble the SC at the interface between homolog pairs, as revealed by DAPI staining of DNA and immunostaining with antibodies against the core SC component, SYP-1 (MacQueen *et al*, 2002) (Figure 2C). Furthermore, six DAPI-stained bivalent chromosomes are detectable at diakinesis in *atl-1(tm853)* oocyte nuclei, indicative of successful crossover recombination (Figure 2C). Thus, *at1-1* is dispensable for SC assembly and crossover recombination during meiotic prophase I.

atl-1 is required for the S-phase checkpoint

It has been proposed that the primary role of ATR in human cells is to respond to problems encountered during S-phase that culminate in replication fork stalling, whereas ATM primarily responds to DSBs (Shiloh, 2003; Kastan and Bartek, 2004). The mitotic defects in *atl-1* and *rad-5/clk-2* mutants are consistent with shared roles as checkpoint sensors required for stabilizing stalled replication forks during S-phase. Since *rad-5/clk-2* is the only *C. elegans* gene so far shown to be essential for the S-phase checkpoint (Ahmed *et al*, 2001), we next determined the integrity of this response in *atl-1* and *atm-1* mutants by subjecting L4 staged animals to treatment with hydroxyurea (HU), an inhibitor of ribonucleotide reductase that leads to replication fork stalling. Consistent with previous reports (Ahmed *et al*, 2001), HU treatment of wild-type (N2) animals leads to S-phase arrest that manifests as enlarged nuclei with an overall reduction in the number of nuclei in the mitotic compartment of the germline (72.3 ± 2.4 versus 12.6 ± 0.8 after treatment, $P < 0.01$). Cell cycle arrest is also evident in animals RNAi depleted for the *C. elegans* ATM homolog, *atm-1* (67.4 ± 3.6 versus 16.8 ± 1.4 after treatment, $P < 0.01$), whereas *rad-5/clk-2* mutants fail to arrest cell cycle progression after HU-treatment (Figure 3A) (Ahmed *et al*, 2001). Similar to *rad-5/clk-2* mutants, mitotic nuclei in *atl-1* mutants also fail to arrest following HU-treatment as revealed by an absence of enlarged mitotic nuclei and no measurable decrease in the number of nuclei in the mitotic compartment when compared with untreated animals (Figure 3A) (49.7 ± 2.6 versus 48.4 ± 4.8 after treatment, $P < 0.5$). The same results was also obtained with *atl-1(RNAi)* (Supplementary Figure S2B). These results indicate that both *atl-1* and *rad-5/clk-2*

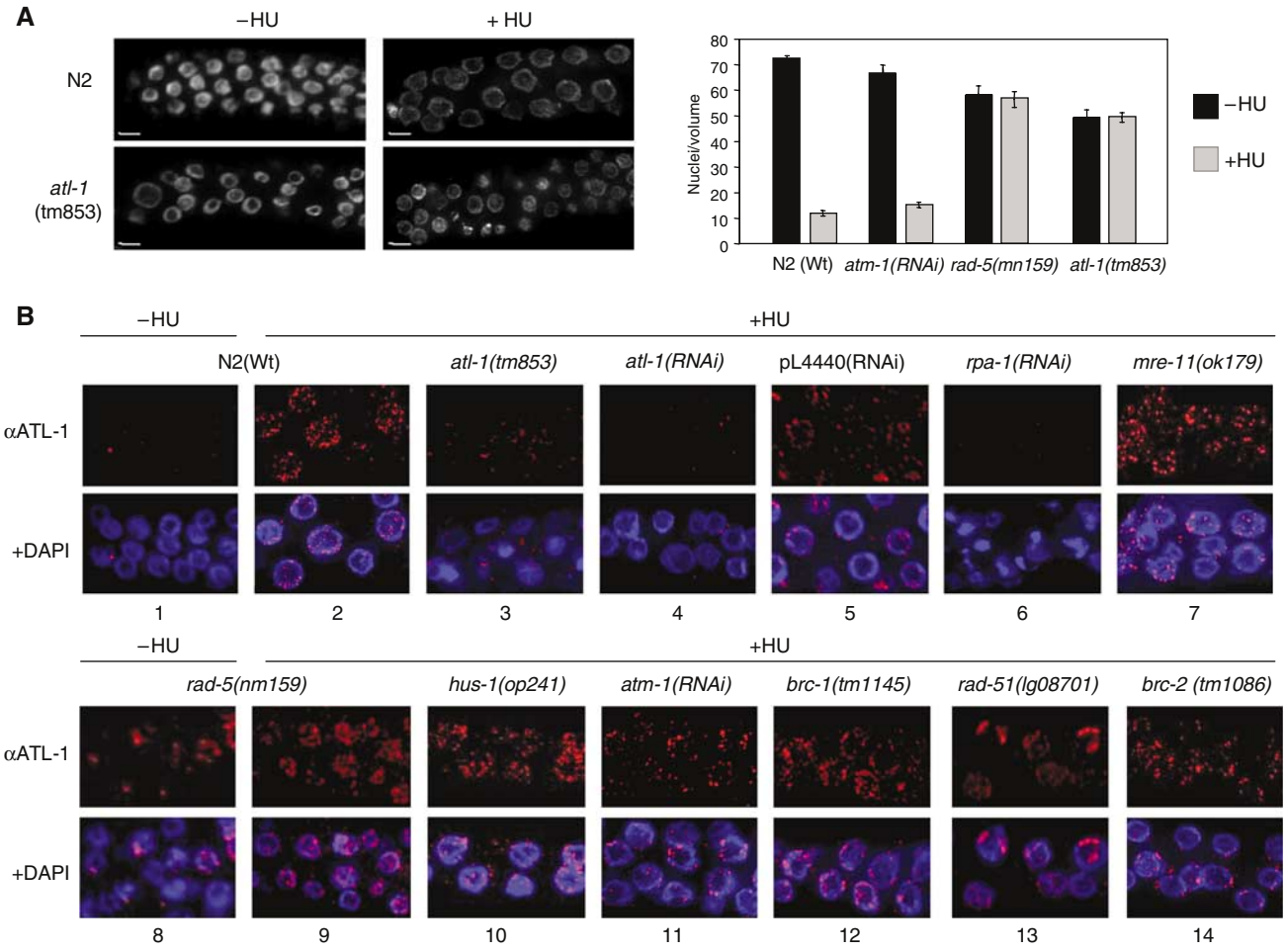

Figure 3 ATL-1 is required for cell cycle arrest after HU and is recruited to stalled replication forks in an *rpa-1* dependent manner. (**A**) Representative images of a single focal plane through the mitotic region of the germline from animals of the indicated genotype counterstained with DAPI, with and without HU treatment (scale bar = 5 μm). The graph on the right shows quantification of HU-induced cell cycle arrest of mitotic germline nuclei that was determined in animals of the indicated genotype by scoring the number of nuclei in a volume of 54 000 μm^3 16 h after exposure of L4 stage animals to 40 mM hyrdroxyurea, as previously described (Ahmed *et al*, 2001). At least 10 germlines were scored for each experiment. (**B**) Representative images of ATL-1 staining of fixed mitotic nuclei for the indicated genotypes following 16 h of HU treatment (quantification of this data is shown in Supplementary Figure S3C and ATL-1 staining without treatment is shown in Supplementary Figure S3A).

are components of the S-phase checkpoint required to induced cell cycle arrest in response to replication fork stalling. In contrast, *atm-1* is dispensable for the S-phase checkpoint response.

ATL-1 is recruited to stalled replication forks by RPA-1/ssDNA

To further explore the role of ATL-1 in responding to S-phase insults, we raised antibodies to examine ATL-1 localization in cells arrested during DNA replication by HU-treatment. Under normal growth conditions, germline nuclei from wild-type (N2) animals are devoid of any detectable ATL-1 staining (Figure 3B1). In contrast, ATL-1 is detected in multiple nuclear foci in mitotic germline nuclei arrested in S-phase following HU-treatment, but is absent in nuclei at all stages of meiotic prophase (Figure 3B2; data not shown) and is dramatically reduced in *atl-1(tm853)* mutants or in animals subjected to *atl-1* RNAi depletion (Figure 3B3 and 4). This result indicates that ATL-1 localizes to sites of replication fork stalling in mitotic cells after HU treatment.

In order to define the position and function of ATL-1 within the signalling cascade required to trigger the S-phase checkpoint in *C. elegans*, we analyzed ATL-1 focus formation in mutants defective for several DDRs genes, including *rpa-1*, *mre-11*, *atm-1*, *rad-5/clk-2*, *hus-1*, *atm-1*, *brc-1*, *brd-1*, *rad-51* and *brc-2* (Ahmed *et al*, 2001; Chin and Villeneuve, 2001; Hofmann *et al*, 2002; Boulton *et al*, 2004; Martin *et al*, 2005). RPA-1 and ATL-1 focus formation following HU-treatment is abolished in animals subjected to *rpa-1(RNAi)* depletion (Supplementary Figure S3B; Figure 3B6), indicating that RPA-1 is required for ATL-1 recruitment to stalled replication forks, a result in agreement with previous reports in mammalian cells (Zou and Elledge, 2003). In untreated *rad-5/clk-2* mutants, ATL-1 foci accumulate in the majority of nuclei within the mitotic zone (Figure 3B8), consistent with the presence of ssDNA and DSBs within this region (Figure 2B). ATL-1 foci also increase in number in *rad-5/clk-2* mutants after HU treatment (Figure 3B9). These data indicate that *rad-5/clk-2* is dispensable for recruitment of ATL-1 to stalled replication forks, despite being defective for the S-phase

checkpoint. Animals harboring mutations in *mre-11* or *hus-1* or animals depleted for *atm-1* by RNAi are also competent for ATL-1 focus formation after HU (Figure 3B7, 10 and 11) (Chin and Villeneuve, 2001). Furthermore, ATL-1 foci form as normal after HU-treatment in mutants defective for DSB repair and recombinational restart of collapsed replication forks, including *brc-1, brd-1*, *rad-51* and *brc-2* (Boulton *et al*, 2004; Martin *et al*, 2005) (Figure 3B12–14; Supplementary Figure S3D). Together, these data indicate that ATL-1 recruitment to stalled replication forks does not require *rad-5/clk-2*, *mre-11*, *atm-1*, *hus-1* or DSB repair genes, but does require *rpa-1*.

ATL-1 is recruited to processed DSBs in an rpa-1 and mre-11 dependent manner

It is currently unclear if ATR cooperates with ATM in the checkpoint response to DSBs generated following IR-treatment. To examine this possibility in *C. elegans*, we next assessed whether *atl-1* has any role in the response to IR as has been previously suggested using *atl-1* RNAi (Boulton *et al*, 2002). Following exposure to an intermediate dose of IR (75 Gy) for *C. elegans* (Ahmed *et al*, 2001; Chin and Villeneuve, 2001; Hofmann *et al*, 2002; Boulton *et al*, 2004; Martin *et al*, 2005), ATL-1 responds by accumulating at discrete nuclear foci at sites of DSBs (Figure 4A2). ATL-1 foci are first detected in wild-type N2 animals 30thinsp;min after IR-treatment and persist for more than 8 h (data not shown). This signal corresponds to ATL-1 protein as IR-induced foci are absent in *atl-1(tm853)* mutants (Figure 4A3).

To examine the genetic requirements for ATL-1 recruitment to IR-induced DSBs, we assessed ATL-1 focus formation in several mutants required for the DNA damage checkpoint (*rpa-1*, *mre-11*, *atm-1*, *hus-1* and *rad-5*) (Ahmed *et al*, 2001; Chin and Villeneuve, 2001; Hofmann *et al*, 2002). RNAi depletion of *rpa-1* abolishes IR-induced ATL-1 focus formation (Figure 4A5), indicating that ATL-1 recruitment to DSBs and to stalled replication forks are both dependent on the formation of RPA-ssDNA complexes. Moreover, mutants defective for the *mre-11* component of the MRN complex are also severely defective for ATL-1 focus formation after IR-treatment (Figure 4A6), revealing a distinct difference in the genetic requirements for ATL-1 focus formation at stalled replication forks versus ATL-1 recruitment to IR-induced

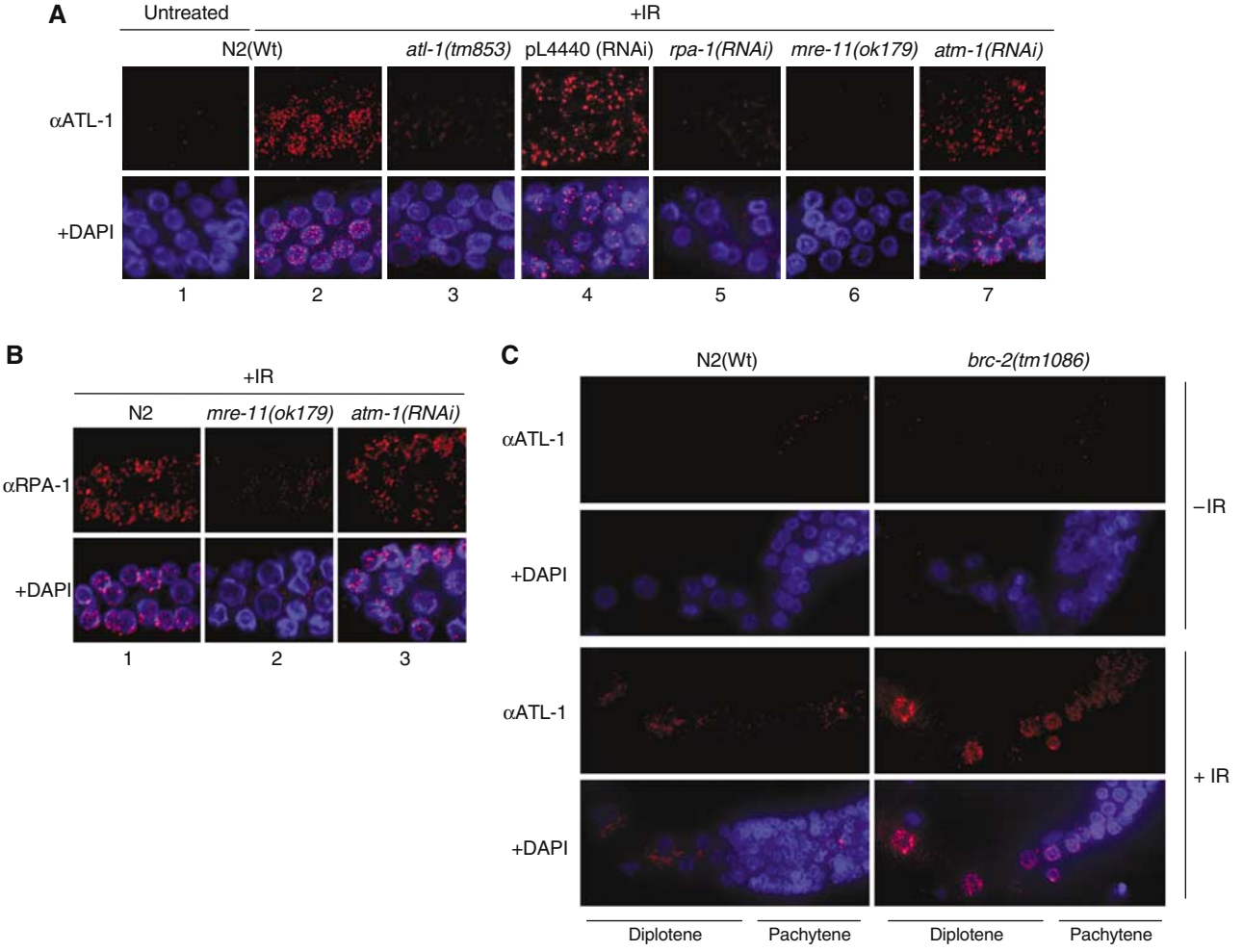

Figure 4 ATL-1 is recruited to processed DSBs following exposure to IR in an *rpa-1* and *mre-11* dependent manner. (**A**) ATL-1 staining of fixed germline nuclei from N2(Wt) animals before and after 1 h post-IR-treatment (75 Gy) and in animals of the indicated genotypes 1 h after IR-treatment (75 Gy). (**B**) RPA-1 staining of fixed mitotic nuclei for the indicated genotypes 1 h after IR-treatment (75 Gy). (**C**) ATL-1 staining of fixed diplotene nuclei during meiotic prophase for the indicated genotypes before and 1 h after IR-treatment (75 Gy). All images shown are representative of fixed germline staining with the respective antibodies.

DSBs. One plausible interpretation of these data is that ATL-1 is recruited by RPA-1 to ssDNA generated by replication stress or following resection of DSBs following IR. The observations that nuclease deficient alleles of Mre11 are sensitive to IR (Moreau *et al*, 1999), confer moderate defects in processing meiosis specific DSBs (Tsubouchi and Ogawa, 1998; Moreau *et al*, 1999) and display reduced resection of HO DSBs (Tsubouchi and Ogawa, 1998; Moreau *et al*, 1999) raises the possibility that *C. elegans mre-11* may regulate processing of IR-induced DSBs to generate ssDNA overhangs bound by RPA. Consistent with this hypothesis, Figure 4B2 shows that *mre-11* mutants are severely impaired for RPA-1 focus formation at sites of DSBs following IR-treatment. The majority of *mre-11* mutant germlines have no detectable RPA-1 or ATL-1 staining. However in a few germlines, we observed a small number of RPA-1 and ATL-1 foci in a subset of nuclei (data not shown). Recent studies have shown that the MRN complex recruits ATM to sites of DSBs (Falck *et al*, 2005; Lee and Paull, 2005). Given our finding that ATL-1 recruitment to DSBs also requires *mre-11*, we next assessed the role of the *atm-1* in the recruitment of ATL-1 to IR-induced DSBs. Contrary to *mre-11* mutants, loss of *atm-1* does not affect ATL-1 focus formation or the formation of RPA–ssDNA complexes at DSBs following IR-treatment (Figure 4A7 and B3). Together, these results indicate that *mre-11*, but not *atm-1,* are required for RPA-1 and ATL-1 recruitment to DSBs and also suggests that the predominant mechanism for DSB resection relies on *mre-11* function, although DSBs can be resected inefficiently in their absence.

ATL-1 is recruited to persistent DSBs in mitotic and meiotic cells

To analyze the response of ATL-1 to an alternative source of DSBs, we monitored recruitment of ATL-1 following phleomycin treatment. Although ATL-1 foci are detectable, the dose and conditions required to induce DSB formation in the *C. elegans* germline, as revealed by RAD-51 focus formation, are excessive (25 mg/ml for 4 days), indicating that phleomycin is not a satisfactory method for producing DSB in this system (data not shown). Since we have previously reported that *C. elegans* BRCA2 mutants (*brc-2*), defective for nuclear localization and recruitment of RAD-51 to DSBs, exhibit RPA-1 foci at persistent DSBs in late pachytene and diplotene stages of meiotic prophase (Martin *et al*, 2005), we also monitored ATL-1 recruitment to DSBs in meiotic cells. In contrast to wild-type (N2) animals, ATL-1 foci accumulate in *brc-2* mutants in pachytene and diplotene nuclei similar to that previously reported for RPA-1 (Figure 4C; Martin *et al*, 2005). These data indicate that ATL-1 recruitment to DSBs is not restricted to mitotic cells, but can also respond to persistent DSBs in meiotic prophase nuclei.

In *brc-1*, *brd-1*, *rad-51* and *brc-2* mutants, IR-induced DSBs persist due to defects in DSB repair (Boulton *et al*, 2004; Martin *et al*, 2005). ATL-1 nuclear foci are elevated in number in the mitotic zone of these mutants following IR (Supplementary Figure S4A and B). ATL-1 foci also persist in *rad-5* and *hus-1* mutants (Ahmed *et al*, 2001; Hofmann *et al*, 2002), which are both compromised for the checkpoint response to IR (Supplementary Figure S4C). These data suggest that ATL-1 responds to persistent and/or irreparable DSBs.

atl-1, atm-1 and rad-5/clk-2 are required for the checkpoint response following IR

Our observation that ATL-1 is recruited to sites of DSBs following IR-treatment raises the possibility that like *atm-1* and *rad-5/clk-2* mutants (Ahmed *et al*, 2001), *atl-1* may be required for checkpoint responses to DSBs, including the induction of cell cycle arrest in the mitotic compartment or triggering apoptosis of pachytene nuclei during meiotic prophase (Gartner *et al*, 2000). Similar to *atm-1(RNAi)* and the *rad-5/clk-2* mutant, the *atl-1(tm853)* mutant is severely compromised for mitotic cell cycle arrest following IR (Figure 5A), with no measurable difference in the number or size of mitotic nuclei before or after treatment (49.7 ± 2.6 versus 49.3 ± 1.8, $P < 0.1$). Following IR-treatment of wild-type (N2) animals, pachytene cells with persistent DNA damage undergo checkpoint dependent apoptosis (Figure 5B), showing a progressive increase in the number of apoptotic corpses over 12–36 h ($P < 0.001$ versus nonirradiated worms). In contrast to wild type, but similar to *atm-1(RNAi)* and the *rad-5/clk-2* mutant, after exposure to 75 Gy of IR, no measurable increase in the number of apoptotic corpses is detectable in the *atl-1*(*tm853*) mutant (at 12 h the apoptotic corpses in the wild type are 6 ± 0.1 versus the *atl-1* 0.8 ± 0.01; at 24 h 7.9 ± 0.3 versus 0.73 ± 0.1; at 36 h 4.9 ± 0.5 versus 1.7 ± 0.3. $P < 0.001$ each time). The same results was also obtained with *atl-1(RNAi)* (Supplementary Figure S2C). These results indicate that *atm-1*, *rad-5/clk-2* and *atl-1* are required for checkpoint-dependent cell cycle arrest and apoptosis in response to IR.

atl-1 triggers apoptosis via cep-1/egl-1 in response to IR

In *C. elegans*, DNA-damage induced apoptosis of pachytene cells requires the core apoptotic machinery (CED-9/4/3) and the proapoptotic gene *egl-1*, whose expression is induced following IR-treatment in a *cep-1* (*C. elegans* p53) dependent manner (Derry *et al*, 2001; Schumacher *et al*, 2001). To determine if *atl-1* triggers apoptosis following IR-treatment through a pathway dependent upon *cep-1*, we monitored the transcriptional activation of a *Pegl-1::gfp* transcriptional reporter (Hofmann *et al*, 2002) in animals subjected to *atl-1(RNAi)* depletion. As previously reported (Hofmann *et al*, 2002), GFP expression is induced in mitotic nuclei of RNAi control animals following IR-treatment (Figure 5C), with 35/45 germlines showing GFP-expressing nuclei. In contrast, no detectable expression from the *Pegl-1::gfp* reporter is observed in mitotic nuclei in animals subjected to *atl-1(RNAi)* after IR-treatment (Figure 5C), with 1/45 germlines showing GFP-expressing nuclei. Collectively, these results indicate that ATL-1 triggers *cep-1* and *egl-1* dependent apoptosis of pachytene cells following IR-treatment.

Discussion

This study reveals that *atl-1* and *rad-5/clk-2* prevent genomic instability and mitotic catastrophe during normal cell cycle progression and function in the checkpoint response to replication stress to bring about cell cycle arrest during S-phase. It has been proposed that the essential function of the S-phase checkpoint is to prevent fork collapse during replication fork pausing (Lopes *et al*, 2001; Tercero and Diffley, 2001). The accumulation of ssDNA and DSBs in *atl-1* and *rad-5/clk-2* mutants, specifically in mitotically dividing cells, is consistent with the accumulation of collapsed

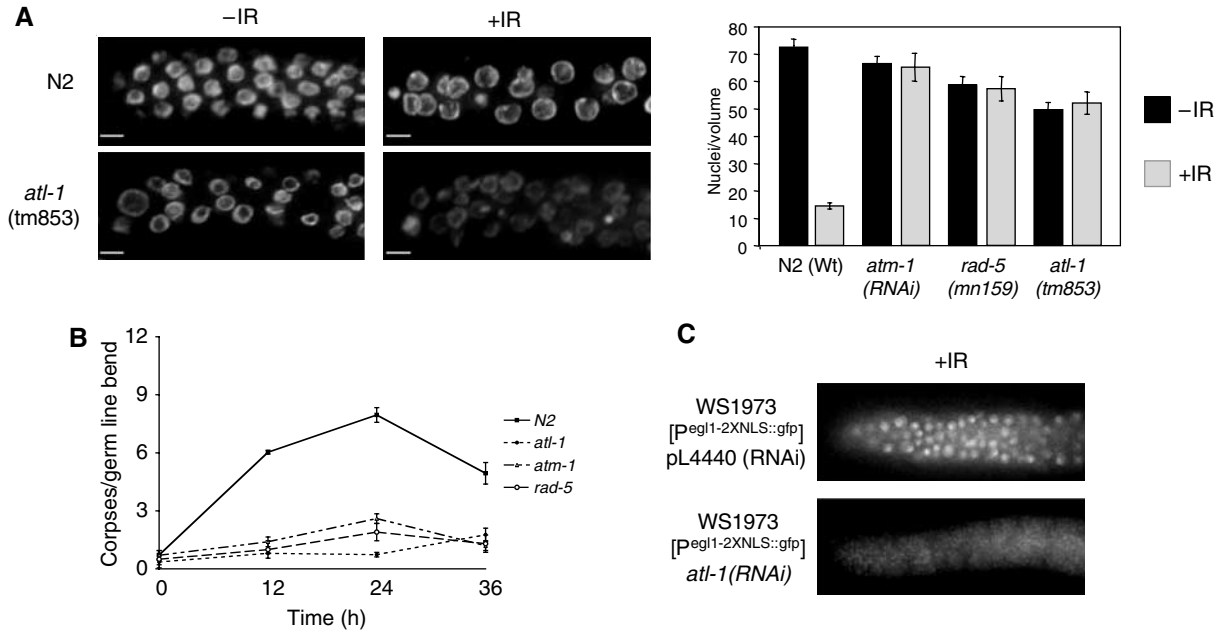

Figure 5 *atl-1* is required for checkpoint-dependent cell cycle arrest and apoptosis following IR via the *cep-1/egl-1* proapoptotic pathway. (**A**) Representative images of a single focal plane through the mitotic region of the germline from animals of the indicated genotype counterstained with DAPI following IR-treatment (scale bar = 5 μm). The graph on the right shows quantification of IR-induced cell cycle arrest of mitotic germline nuclei in animals of the indicated genotype that was determined by scoring the number of nuclei in a volume of 54 000 μm^3 12 h after exposure of L4 stage animals to 75 Gy IR, as previously described (Gartner *et al*, 2000). Error bars indicate standard error of mean from at least ten germlines for each experiment. (**B**) Germ cell apoptosis was measured by differential interference contrast (DIC) microscopy in animals of the indicated genotype at the indicated time points post IR-treatment. Error bars indicate standard error of mean from at least ten germlines for each time point. (**C**) Representative images of GFP expression from the *Pegl-1*::*gfp* transcriptional reporter (Hofmann *et al*, 2002) 30 h after IR treatment (120 Gy) in animals subjected to L4440 RNAi (control) and *atl-1(RNAi)*.

replication forks in these mutants. A role for *atl-1* in stabilizing stalled replication forks is further supported by our finding that ATL-1 is recruited to sites of replication forks pausing. While this role is predicted for ATL-1, based on analogy to Mec1p in yeast, this was not known for RAD-5/CLK-2. It is currently unclear how RAD-5/CLK-2 functions in the S-phase checkpoint and prevents replication fork collapse (Ahmed *et al*, 2001). However, it is intriguing to note that Tel2p, the yeast homolog of RAD-5/CLK-2, interacts with the Cdc7p kinase (Uetz *et al*, 2000), a component of the replisome required for late origin firing, for the normal checkpoint response to HU-treatment and for trans-lesion synthesis as part of the RAD6 epistasis group (Bousset and Diffley, 1998; Weinreich and Stillman, 1999; Pessoa-Brandao and Sclafani, 2004). While it remains to be seen if RAD-5/CLK-2 associates with CDC-7 kinase in *C. elegans*, defects in regulating CDC-7 could impact on fork stability. Further studies of RAD-5/CLK-2 are likely to provide important insight into the S-phase checkpoint and the mechanism through which it functions with ATL-1 to stabilize stalled replication forks.

It has been shown that ATRIP, the interacting partner of ATR, senses DNA damage by recognizing and binding to RPA-ssDNA complexes that arise during replication stress or following DNA damage (Zou and Elledge, 2003). Consistent with these observations, we find that ATL-1 is also recruited to stalled replication forks by RPA-1/ssDNA (Figure 3B), indicating that the mechanism of ATL-1 recruitment and its activation at stalled replication forks is conserved. A *C. elegans* homolog of ATRIP (Zou and Elledge, 2003; Ball *et al*, 2005; Falck *et al*, 2005) has not been identified to date so this remains to be formally shown in the nematode. Although *rad-5/clk-2* mutants are compromised for the S-phase checkpoint and exhibit evidence of replication fork collapse, these mutants still remain competent for ATL-1 recruitment to stalled replication forks (Figure 3B). This result suggests that recruitment of ATL-1 to stalled replication forks is not sufficient to prevent collapse of stalled forks and also indicates that ATL-1 functions upstream of RAD-5/CLK-2 in the S-phase checkpoint. Rather, we propose that ATL-1 and RAD-5/CLK-2 function together or in nonredundant parallel pathways to stabilize stalled replication forks (Figure 6A).

We also show that ATL-1 is recruited to IR-induced DSBs in both mitotic and meiotic cells, suggesting that ATL-1 also responds to DSBs even in cells outside of S-phase. Our analyses highlight a distinct difference in the mechanistic requirements for ATL-1 focus formation at stalled replication forks versus ATL-1 recruitment to IR-induced DSBs. Specifically, we have shown that ATL-1 recruitment to IR-induced DSBs is dependent upon *mre-11* and *rpa-1* (Figure 4A). In contrast, the generation or exposure of ssDNA bound by RPA that signals ATL-1 recruitment following replication stress does not require the action of either *atm-1* or *mre-11* (Figure 3B). We propose that DSBs generated following IR-treatment require prior processing to generate ssDNA overhangs that become bound by RPA and recruit and activate ATL-1. What is particularly surprising is that processing of DSBs required to recruit and activate ATL-1 is genetically dependent on *mre-11*, but not on *atm-1*. How MRE-11 regulates DSB processing is not clear. One possible explanation is that MRE-11 recruits an exonuclease that mediates DSB processing to generate a resected ssDNA end bound by RPA. Alternatively, MRE-11 possesses exonuclease activity *in vitro*

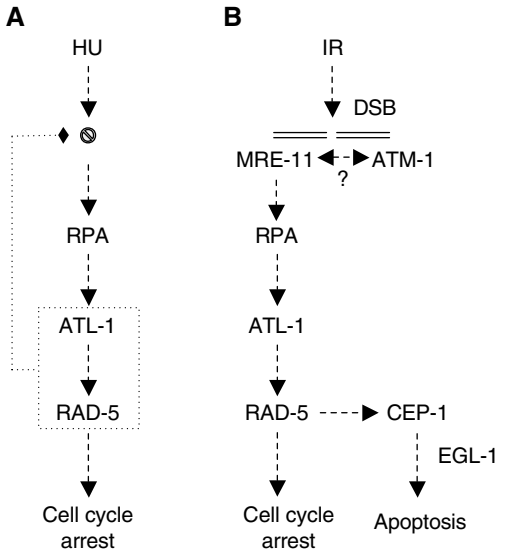

Figure 6 A model for ATL-1 activation in response to replication fork stalling and following processing of DSBs. (**A**) RPA-ssDNA complexes generated following replication fork pausing/stalling following hydroxyurea (HU) treatment recruit ATL-1. ATL-1 and RAD-5/CLK-2 are both required to stabilize stalled replication forks and to activate the S-phase checkpoint to transiently arrest the cell cycle to provide time to restart DNA synthesis. (**B**) MRE-11 is recruited to DSBs generated following IR-treatment. Once recruited, MRE-11 is believed to recruit ATM-1 based on studies in mammalian cells and also regulates DSB processing. RPA-ssDNA complexes generated by DSB resection recruit ATL-1. Together, ATL-1, RAD-5/CLK-2 and ATM-1 cooperate to induce cell cycle arrest or apoptosis via the *cep-1/egl-1* pathway.

and could itself be responsible for DSB processing (Moreau *et al*, 1999; Paull and Gellert, 1999).

The observation that ATR is recruited to DSBs has led to speculation that it may function with ATM in the checkpoint response to DSBs. However, the essential nature of ATR has precluded the direct analysis of its role in this response. Maternal rescue of the *atl-1* mutant circumvents this problem and has allowed us to assess the role of *atl-1* in the checkpoint response to DSBs generated following IR-treatment. Our data show that *atl-1*, *atm-1* and *rad-5/clk-2* are all required for checkpoint dependent cell cycle arrest and *cep-1*(p53)*/egl-1* mediated apoptosis in response to IR (Figures 5 and 6B). Moreover, our phenotypic comparison of *atm-1*, *atl-1* and *atm-1*; *atl-1* double mutants strongly suggest that ATM-1 and ATL-1 function in a common pathway, rather than in parallel or partially parallel pathways (Supplementary Figure S5). Our data suggest that the conventional model in which ATM mediates the checkpoint response to DSBs, whereas ATR responds to UV damage or replication stress may be an oversimplification. Taken together with recent findings, we hypothesize that in response to DSBs, MRE-11 (MRN complex) is targeted to DSBs where it facilitates recruitment of ATM-1 (ATM; Falck *et al*, 2005; Lee and Paull, 2005). While the role of the MRN complex in ATM recruitment to DSBs is widely accepted in mammalian cells this has not been formally shown in *C. elegans* and requires further study. Our findings indicate that MRE-11 also regulates DSB processing to generate RPA-ssDNA complexes that target ATL-1 recruitment to DSBs. Once recruited, ATL-1 (ATR), together with RAD-5/CLK-2 and ATM-1, are required to activate the checkpoint response to induce cell cycle arrest or apoptosis (Figure 6B).

Materials and methods

Strains and culture conditions

C. elegans strains were cultured and maintained using standard procedures. The following strains were kindly provided by the *Caenorhabditis* Genetics Centre (University of Minnesota, St Paul, MN), including wild-type Bristol N2, *mre-11(ok179)* (Chin and Villeneuve, 2001), *rad-51(lg08701)*, *brc-1(tm1145)*, *rad5(mn159)* (Ahmed *et al*, 2001), *hus-1(op241)* (Hofmann *et al*, 2002), *brd-1(dw1)*, *brc-2(tm1086)* (Martin *et al*, 2005) and WS1973 *[Pegl-1_2nls::gfp]* (Hofmann *et al*, 2002) were described previously. *atl-1(tm853)* was generated and kindly provided by Shoehi Mitani of the National Bioresource Project for the nematode, Japan. Deletions were outcrossed six times with the wild-type Bristol N2 and then balanced with JK2663 [*dpy-11 (e224) mes-4 (bn67)* V/nT1(qIs50) IV;V]. The phenotypes we describe for *atl-1* cosegregate with the *tm853* mutation. *tm853/+* hets are wild type for all of the assays we have described, whereas *atl-1(RNAi)* to a large extent recapitulates the *tm853* homozygous mutant phenotype (Supplementary Figure S2). RNA interference (RNAi) depletion of *rpa-1*, *atm-1* and *atl-1* was performed by the feeding method described previously (Boulton *et al*, 2002). Hydroxyurea (HU) treatment was performed as previously described (Ahmed *et al*, 2001). L4 larvae were transferred to plates with 40 mM final HU for 16 and 24 h prior to analysis. To assay radiation-induced germ-cell death, apoptotic cell corpses were measured 0, 12, 24 and 36 h after irradiation using Nomarski optics, as previously described (Gartner *et al*, 2000; Boulton *et al*, 2002). RNAi experiments were performed in the RNAi sensitive *C. elegans* strain, *rrf-3(pk1426)* as previously described (Simmer *et al*, 2002). *atm-1*, *atl-1* and *rpa-1* RNAi was found to be more penetrant in *rrf-3* strains compared with previous studies using wild-type N2 strains (Boulton *et al*, 2002).

Gateway recombinational cloning

ORF specific primers compatible with the Gateway® system (http://www.invitrogen.com) were designed to full-length *rpa-1* (F18A1.5) and *atm-1* (Y48G1BL.2) genes, PCR amplified and cloned into the p221 Entry vector as previously described (Boulton *et al*, 2002). The cloned open reading frames were transferred by LR destination cloning into L4440-dest for RNAi by feeding.

ATL-1 antibodies

An N-terminal synthetic peptide corresponding to the 20 first amino acids (CTAKKYVTQKEFNRQKMKFL) of ATL-1 was generated by the Peptide Synthesis Laboratory, Cancer Research UK, and used to generate rabbit anti-ATL-1 polyclonal antibodies. Animals were immunized (Harlan Sera Labs, Loughborough, UK) with 1 mg of each peptide coupled to activated keyhole limpet hemocyanin (Pierce, Rockford, III). Affinity purified antibodies were tested by Western blotting against recombinant proteins expressed in *Escherichia coli* and subsequently by immunofluorescence in N2(Wt) and *atl-1(tm853)* to test for specificity. The signal observed following HU and IR-treatment is abolished by *atl-1(RNAi)*, by incubation with a competitor peptide corresponding to the epitope recognized by the ATL-1 antibody, and is dramatically reduced in *atl-1(tm853)*.

Cytological preparation and immunostaining

Gravid hermaphrodites were transferred to 30 µl PBS on a poly-L lysine coated slide (slides were washed in 70% ethanol, then given 2 coats of 100% poly-L-lysine, air drying between each coat). The worms were washed in PBS before transferring to 50 µl 10 mM levamisole. Germlines were extruded by removing the head and tail using a fine gauge needle (27 G). Levamisole was replaced with 1% para-formaldehyde (PFA) in PBS for 10 min and germlines were permeabilized for 5 min in TBSBT (TBS + 0.5% BSA + 0.1% Triton X-100), then washed in TBSB for at least 2 × 5 min, followed by blocking for 30 min. Primary antibodies were diluted in TBSB (1:200 for RAD-51, 1:200 SYP-1, 1:500 RPA-1, 1:500 ATL-1) and incubated overnight at 4°C in a humid chamber. Germlines were subsequently washed at least 3 × 5 min in TBSB before incubation with the secondary antibody for 1–2 h at room temperature (anti-rabbit Cy3 1:10 000; anti-guinea FITC 1:5000 (Sigma)). Finally, germlines were washed at least 3 × 5 min in TBSB before mounting with a coverslip on Vectashield containing DAPI (Vector Laboratories).

Fluorescence microscopy

Deltavision microscopy was used to examine germlines with $\times 40$ or $\times 63$, 1.4 NA Planapochromat lens on an Olympus inverted microscope (IX71), and images captured using SoftWorx computer software (Applied Precision). Three-dimensional data sets were computationally deconvolved, and regions of interest then projected into one dimension. Merged or single color images were recorded using GIMP software.

Supplementary data

Supplementary data are available at *The EMBO Journal* Online.

Acknowledgements

We thank the Bioresource Project for the nematode (Shohei Mitani) for kindly providing *atl-1(tm853)*, E. Randel Hofmann and Michael Hengartner for the WS1973 *[Pegl-2nls::gfp]* strain and the *Caenorhabditis* Genetic Centre and the Sanger Centre for providing *C. elegans* strains and cosmids. We also thank members of the Boulton lab for helpful discussions and to Vincenzo Costanzo, Spencer Collis, Louise Barber, Monica Segurado and Julie Martin for comments on the manuscript. This work was funded by Breast Cancer Campaign (GA3221) and Cancer Research UK.

Competing interests statement

The authors declare that they have no competing financial interests.

References

Abraham RT (2001) Cell cycle checkpoint signaling through the ATM and ATR kinases. *Genes Dev* **15:** 2177–2196

Ahmed S, Alpi A, Hengartner MO, Gartner A (2001) *C. elegans* RAD-5/CLK-2 defines a new DNA damage checkpoint protein. *Curr Biol* **11:** 1934–1944

Ahmed S, Hodgkin J (2000) MRT-2 checkpoint protein is required for germline immortality and telomere replication in *C. elegans*. *Nature* **403:** 159–164

Alderton GK, Joenje H, Varon R, Borglum AD, Jeggo PA, O'Driscoll M (2004) Seckel syndrome exhibits cellular features demonstrating defects in the ATR-signalling pathway. *Hum Mol Genet* **13:** 3127–3138

Aoki H, Sato S, Takanami T, Ishihara T, Katsura I, Takahashi H, Higashitani A (2000) Characterization of Ce-atl-1, an ATM-like gene from *Caenorhabditis elegans*. *Mol Gen Genet* **264:** 119–126

Bakkenist CJ, Kastan MB (2003) DNA damage activates ATM through intermolecular autophosphorylation and dimer dissociation. *Nature* **421:** 499–506

Ball HL, Myers JS, Cortez D (2005) ATRIP binding to replication protein A-single-stranded DNA promotes ATR-ATRIP localization but is dispensable for Chk1 phosphorylation. *Mol Biol Cell* **16:** 2372–2381

Boulton SJ, Gartner A, Reboul J, Vaglio P, Dyson N, Hill DE, Vidal M (2002) Combined functional genomic maps of the *C. elegans* DNA damage response. *Science* **295:** 127–131

Boulton SJ, Martin JS, Polanowska J, Hill DE, Gartner A, Vidal M (2004) BRCA1/BARD1 orthologs required for DNA repair in *Caenorhabditis elegans*. *Curr Biol* **14:** 33–39

Bousset K, Diffley JF (1998) The Cdc7 protein kinase is required for origin firing during S phase. *Genes Dev* **12:** 480–490

Brauchle M, Baumer K, Gonczy P (2003) Differential activation of the DNA replication checkpoint contributes to asynchrony of cell division in *C. elegans* embryos. *Curr Biol* **13:** 819–827

Brown EJ, Baltimore D (2000) ATR disruption leads to chromosomal fragmentation and early embryonic lethality. *Genes Dev* **14:** 397–402

Carney JP, Maser RS, Olivares H, Davis EM, Le Beau M, Yates III JR, Hays L, Morgan WF, Petrini JH (1998) The hMre11/hRad50 protein complex and Nijmegen breakage syndrome: linkage of double-strand break repair to the cellular DNA damage response. *Cell* **93:** 477–486

Chin GM, Villeneuve AM (2001) *C. elegans* mre-11 is required for meiotic recombination and DNA repair but is dispensable for the meiotic G(2) DNA damage checkpoint. *Genes Dev* **15:** 522–534

Cliby WA, Roberts CJ, Cimprich KA, Stringer CM, Lamb JR, Schreiber SL, Friend SH (1998) Overexpression of a kinase-inactive ATR protein causes sensitivity to DNA-damaging agents and defects in cell cycle checkpoints. *EMBO J* **17:** 159–169

Conradt B, Horvitz HR (1998) The *C. elegans* protein EGL-1 is required for programmed cell death and interacts with the Bcl-2-like protein CED-9. *Cell* **93:** 519–529

Cortez D, Guntuku S, Qin J, Elledge SJ (2001) ATR and ATRIP: partners in checkpoint signaling. *Science* **294:** 1713–1716

Costanzo V, Paull T, Gottesman M, Gautier J (2004) Mre11 assembles linear DNA fragments into DNA damage signaling complexes. *PLoS Biol* **2:** E110

de Klein A, Muijtjens M, van Os R, Verhoeven Y, Smit B, Carr AM, Lehmann AR, Hoeijmakers JH (2000) Targeted disruption of the cell-cycle checkpoint gene ATR leads to early embryonic lethality in mice. *Curr Biol* **10:** 479–482

Derry WB, Putzke AP, Rothman JH (2001) *Caenorhabditis elegans* p53: role in apoptosis, meiosis, and stress resistance. *Science* **294:** 591–595

Durocher D, Jackson SP (2001) DNA-PK, ATM and ATR as sensors of DNA damage: variations on a theme? *Curr Opin Cell Biol* **13:** 225–231

Falck J, Coates J, Jackson SP (2005) Conserved modes of recruitment of ATM, ATR and DNA-PKcs to sites of DNA damage. *Nature* **434:** 605–611

Gartner A, Milstein S, Ahmed S, Hodgkin J, Hengartner MO (2000) A conserved checkpoint pathway mediates DNA damage–induced apoptosis and cell cycle arrest in *C elegans*. *Mol Cell* **5:** 435–443

Hengartner MO (2001) Apoptosis: corralling the corpses. *Cell* **104:** 325–328

Hofmann ER, Milstein S, Boulton SJ, Ye M, Hofmann JJ, Stergiou L, Gartner A, Vidal M, Hengartner MO (2002) *Caenorhabditis elegans* HUS-1 is a DNA damage checkpoint protein required for genome stability and EGL-1-mediated apoptosis. *Curr Biol* **12:** 1908–1918

Kastan MB, Bartek J (2004) Cell-cycle checkpoints and cancer. *Nature* **432:** 316–323

Lee JH, Paull TT (2005) ATM activation by DNA double-strand breaks through the Mre11-Rad50-Nbs1 complex. *Science* **308:** 551–554

Lopes M, Cotta-Ramusino C, Pellicioli A, Liberi G, Plevani P, Muzi-Falconi M, Newlon CS, Foiani M (2001) The DNA replication checkpoint response stabilizes stalled replication forks. *Nature* **412:** 557–561

MacQueen AJ, Colaiacovo MP, McDonald K, Villeneuve AM (2002) Synapsis-dependent and -independent mechanisms stabilize homolog pairing during meiotic prophase in *C. elegans*. *Genes Dev* **16:** 2428–2442

Martin JS, Winkelmann N, Petalcorin MI, McIlwraith MJ, Boulton SJ (2005) RAD-51-dependent and -independent roles of a *Caenorhabditis elegans* BRCA2-related protein during dna double-strand break repair. *Mol Cell Biol* **25:** 3127–3139

Moreau S, Ferguson JR, Symington LS (1999) The nuclease activity of Mre11 is required for meiosis but not for mating type switching, end joining, or telomere maintenance. *Mol Cell Biol* **19:** 556–566

O'Driscoll M, Ruiz-Perez VL, Woods CG, Jeggo PA, Goodship JA (2003) A splicing mutation affecting expression of ataxia-telangiectasia and Rad3-related protein (ATR) results in Seckel syndrome. *Nat Genet* **33:** 497–501

Paull TT, Gellert M (1999) Nbs1 potentiates ATP-driven DNA unwinding and endonuclease cleavage by the Mre11/Rad50 complex. *Genes Dev* **13:** 1276–1288

Pessoa-Brandao L, Sclafani RA (2004) CDC7/DBF4 functions in the translesion synthesis branch of the RAD6 epistasis group in *Saccharomyces cerevisiae*. *Genetics* **167:** 1597–1610

Schumacher B, Hanazawa M, Lee MH, Nayak S, Volkmann K, Hofmann R, Hengartner M, Schedl T, Gartner A (2005) Translational repression of *C. elegans* p53 by GLD-1 regulates DNA damage-induced apoptosis. *Cell* **120:** 357–368

Schumacher B, Hofmann K, Boulton S, Gartner A (2001) The *C. elegans* homolog of the p53 tumor suppressor is required for DNA damage-induced apoptosis. *Curr Biol* **11:** 1722–1727

Shechter D, Costanzo V, Gautier J (2004) ATR and ATM regulate the timing of DNA replication origin firing. *Nat Cell Biol* **6:** 648–655

Shiloh Y (2003) ATM and related protein kinases: safeguarding genome integrity. *Nat Rev Cancer* **3:** 155–168

Simmer F, Tijsterman M, Parrish S, Koushika SP, Nonet ML, Fire A, Ahringer J, Plasterk RH (2002) Loss of the putative RNA-directed RNA polymerase RRF-3 makes *C. elegans* hypersensitive to RNAi. *Curr Biol* **12:** 1317–1319

Tercero JA, Diffley JF (2001) Regulation of DNA replication fork progression through damaged DNA by the Mec1/Rad53 checkpoint. *Nature* **412:** 553–557

Tsubouchi H, Ogawa H (1998) A novel mre11 mutation impairs processing of double-strand breaks of DNA during both mitosis and meiosis. *Mol Cell Biol* **18:** 260–268

Uetz P, Giot L, Cagney G, Mansfield TA, Judson RS, Knight JR, Lockshon D, Narayan V, Srinivasan M, Pochart P, Qureshi-Emili A, Li Y, Godwin B, Conover D, Kalbfleisch T, Vijayadamodar G, Yang M, Johnston M, Fields S, Rothberg JM (2000) A comprehensive analysis of protein-protein interactions in *Saccharomyces cerevisiae*. *Nature* **403:** 623–627

Weinreich M, Stillman B (1999) Cdc7p-Dbf4p kinase binds to chromatin during S phase and is regulated by both the APC and the RAD53 checkpoint pathway. *EMBO J* **18:** 5334–5346

Wright JA, Keegan KS, Herendeen DR, Bentley NJ, Carr AM, Hoekstra MF, Concannon P (1998) Protein kinase mutants of human ATR increase sensitivity to UV and ionizing radiation and abrogate cell cycle checkpoint control. *Proc Natl Acad Sci USA* **95:** 7445–7450

Zou L, Elledge SJ (2003) Sensing DNA damage through ATRIP recognition of RPA-ssDNA complexes. *Science* **300:** 1542–1548